Field-grown *ictB* tobacco transformants show no difference in photosynthetic efficiency for biomass relative to wildtype

Ursula M. Ruiz-Vera[1,*,¶], Liana G. Acevedo-Siaca[1,*,#], Kenny L. Brown[2,&], Chidi Afamefule[2], Hussein Gherli[2], Andrew J. Simkin[3,4], Stephen P. Long[1,5], Tracy Lawson[2], Christine Raines[2]

*Denotes equal first authorship

Corresponding author: rainc@essex.edu

[1] Carl R. Woese Institute for Genomic Biology, University of Illinois at Urbana-Champaign, 1206 W Gregory Drive, IL61801, Urbana, IL, USA.

[2] School of Life Sciences, University of Essex, Wivenhoe Park, Colchester, CO4 3SQ, UK.

[3] School of Biosciences, University of Kent, Canterbury CT2 7NJ, UK.

[4] Crop Science and Production Systems, NIAB-EMR, New Road, East Malling, Kent ME19 6BJ, UK

[5] Lancaster Environment Centre, University of Lancaster, Lancaster, UK.

PRESENT

[¶] Bayer CropScience LLC, Bayer Marana Greenhouse, 9475 N Sanders Rd, Tucson, AZ 85743, USA.

[#] International Maize and Wheat Improvement Center (CIMMYT), México-Veracruz, El Batán Km. 45, 56237 Mexico

[&] N2 Applied AS, Hagaløkkveien 7, 1383 Asker, Norway

AUTHOR EMAILS:

Ursula M. Ruiz-Vera: ruizver1@illinois.edu ; ursularuizvera@gmail.com ; 0000-0003-1890-967X

Liana G. Acevedo-Siaca: l.acevedo@cgiar.org ; 0000-0003-3903-0402

Kenny L. Brown: kennylbrown92@gmail.com ; 0000-0002-0587-2698

Chidi Afamefule: chidi.afamefule@essex.ac.uk ; 0000-0002-6412-7903

Hussein Gherli: hussein.gherli@essex.ac.uk

Andrew J. Simkin: a.simkin@kent.ac.uk ; 0000-0001-5056-1306

Stephen P. Long: slong@illinois.edu ; 0000-0002-8501-7164

Tracy Lawson: tlawson@essex.ac.uk ; 0000-0002-4073-7221

Christine Raines: rainc@essex.ac.uk ; 0000-0001-7997-7823

HIGHLIGHT: Despite previous studies that have shown potential for increased plant productivity through the overexpression of inorganic carbon transporter B (*ictB*), no significant difference was found between field-grown *ictB* expressing tobacco lines and wildtype.

ABSTRACT:

In this study, four tobacco transformants with the overexpression of inorganic carbon transporter B (*ictB*) were screened for photosynthetic performance relative to wild-type (WT) in field-based conditions. The WT and transgenic tobacco plants were evaluated for photosynthetic performance to determine the maximum rate of carboxylation ($V_{c,max}$), maximum rate of electron transport (J_{max}), the photosynthetic compensation point (Γ^*), quantum yield of photosystem II (Φ_{PSII}), and mesophyll conductance (g_m). Additionally, all plants were harvested to compare differences in above-ground biomass. Overall, transformants did not perform better than WT on photosynthesis, biomass, and leaf composition related traits. This is in contrast to previous studies that have suggested significant increases in photosynthesis and yield with the overexpression of *ictB*, although not widely evaluated under field conditions. These findings suggest that the benefit of ictB is not universal and may only be seen under certain growth conditions. While there is certainly still potential benefit to utilizing ictB in the future, further effort must be concentrated on understanding the underlying function of the gene and in which environmental conditions it offers the greatest benefit to crop performance. As of now, it is possible that *ictB* overexpression may be largely favorable in controlled environments, such as greenhouses.

3

INTRODUCTION:

By the year 2050 it is projected that global food supply will need to increase by 50% - 85% to keep up with a growing human population and shifting dietary preferences with greater emphasis on the consumption of animal products (Tilman et al., 2011; Ray et al., 2012, 2013; Long et al., 2015; FAO et al., 2020). As a result, yields of staple crops must increase at a considerably greater rate than today to ensure future food security. Furthermore, future crop varieties must be more sustainable and utilize water and nutrients more efficiently if they are to be environmentally sustainable (Tilman et al., 2011; Foley et al., 2011). While properties such as harvest index and light interception by the canopy have been improved close to their theoretical maximums over the past half century, little improvement has been made to photosynthetic efficiency in crop plants (Zhu et al., 2008). Not only is the current rate of improvement in yield of crops plants insufficient to meet the projected future demand, but it may be stagnating (Long and Ort, 2010; Ray et al., 2012; Long et al., 2015). Increasing photosynthetic efficiency is a little exploited approach that holds great potential promise for improving yield and resource-use efficiencies in crops (Zhu et al., 2008; Long et al., 2015).

Most major crops consumed by humans utilize the C_3 photosynthetic pathway. C_3 crops assimilate CO_2 from the atmosphere inefficiently due to the lack of a carbon concentrating mechanism, several internal resistances to CO_2 diffusion, and because Rubisco is catalytically slow with a slow catalytic rate of CO_2 assimilation in current atmospheric conditions (Tcherkez et al., 2006; Price et al., 2013; Erb and Zarzycki, 2018). The C_3 photosynthetic process is also inefficient in its use of water and nitrogen (Parry et al., 2011; Long et al., 2018). Engineering a carbon concentrating mechanism in C_3 crops, much like those seen in C_4 and cyanobacteria, would significantly reduce these inefficiencies (McGrath and Long, 2014; Long et al., 2015). Indeed, many recent initiatives have aimed to improve C_3 photosynthetic efficiency in crop plants to improve yield and productivity, such as the engineering of a C_4 pathway in rice or constructing cyanobacterial carboxysomes in C_3 chloroplasts (Mitchell and Sheehy, 2006; Long et al., 2018; Ermakova et al., 2020).

The inorganic carbon transporter B (*ictB*) is a highly conserved gene among cyanobacteria that was proposed to be involved in inorganic carbon accumulation in *Synechococcus* PCC 7942 (Bonfil et al., 1998; Lieman-Hurwitz et al.,2003; Price et al., 2013). Previously, it was thought that *ictB* functioned as a carbon pump which could increase CO_2 concentration within the leaf and improve photosynthesis (Lieman-Hurwitz et al., 2002). Since then evidence has been presented showing that the *ictB* protein does not function as a HCO_3^- transporter (Xu et al., 2008; Price et al., 2013), and therefore its function remains unknown (Simkin et al., 2019).

Although the exact function of *ictB* is not yet known, several studies over the past 20 years have indicated that overexpressing *ictB* improves photosynthetic efficiency in C_3 plants. Previously, *Arabidopsis* and tobacco transformants overexpressing *ictB* and grown in a controlled environment were found to have a significantly lower photosynthetic compensation point (Γ^*) than wildtype (WT) (Lieman-Hurwitz et al., 2003). This result suggested that increased *ictB* expression increased [CO_2] at Rubisco, consequently increasing carboxylation rate while competitively inhibiting oxygenation (Lieman-Hurwitz et al., 2003; Hay et al. 2017). In greenhouse-grown tobacco, *ictB* expression led to an increase in the maximum rate of carboxylation ($V_{c, max}$), the maximum rate of electron transport (J_{max}), leaf CO_2 uptake rate (A), and stomatal conductance (g_{sw}) (Simkin et al., 2015). Additionally, *ictB* expression may help boost photosynthetic performance in field conditions. Paddy-grown rice expressing *ictB* had significantly 10.5% higher mesophyll conductance (g_m) and 13.5%

4

higher *A,* compared to wild type (Gong et al., 2015). Field-grown maize also benefited with increases in *A* and carbohydrate production, with increases in yield of up to 9.4% (Koester et al., 2021). Replicated field trials of *ictB* expressing soybean showed significant increases of 25% in g_m, 14% in *A,* and 15% in seed yield relative to wildtype (Hay et al., 2017). Other studies have also noted increases in biomass production (Lieman-Hurwitz et al., 2003; Yang et al., 2008; Simkin et al., 2015). Expression of *ictB* led to faster plant growth and greater accumulation of biomass under low-humidity conditions in Arabidopsis (Lieman-Hurwitz et al., 2003) and higher overall biomass in soybean under water deprivation conditions (Hay et al., 2017). Additionally, biomass increased by 71% in greenhouse-grown *ictB* tobacco transformants (Simkin et al., 2015).

However, these gains may not always translate when grown in field conditions where improvements to crops would be most relevant towards improving food production. Indeed, previous studies have shown that *ictB* expression has not resulted in increased biomass (Gong et al., 2015), except in drought conditions (Hay et al., 2017). Previously, *ictB* tobacco transformants were shown to have increased photosynthetic performance and biomass without affecting water-use efficiency (Simkin et al., 2015). However, these transformants were only screened within the context of a controlled growth environment (Simkin et al., 2015). In the present study, the tobacco transformants developed and utilized in Simkin *et al.* (2015) were grown in field conditions to evaluate their performance. The main objectives of this study were to (i) evaluate photosynthetic performance of *ictB* mutants relative to the wildtype in field conditions, and (ii) assess the potential of *ictB* to improve water-use efficiency in rain-fed field conditions. We subsequently discuss why benefits might be seen in greenhouses and controlled environments for *ictB* transformants but not in field trials.

MATERIALS AND METHODS:

Growing Conditions and Germplasm

Tobacco transformants (ictB1, ictB3, ictB4, and ictB6) were produced at the University of Essex where the *ictB* single construct was placed in tobacco (*Nicotiana tabacum*) cv. Samsun background (Simkin et al., 2015). Tobacco transformants and WT tobacco plants were grown at the Energy Farm at the University of Illinois at Urbana-Champaign in Urbana, Illinois, USA. Seeds were sown into transplant trays on July 9, 2020, and transplanted into the field on August 3, 2020, in a random complete block design in which each genotype was replicated 12 times (Supplementary Figure 1). Temperature (°C) and photosynthetic active radiation (PAR, µmol m^{-2} s^{-1}) were measured through the field season (Supplementary Figure 2). Once in the field, the plants were irrigated as needed to maintain soil moisture near field capacity (Supplementary Figure 2). Measurements were made throughout August - September 2020. A full list of measured traits can be found in Supplementary Table 1.

Gas Exchange Measurements

Leaf CO_2 uptake and modulated chlorophyll fluorescence were measured on the youngest fully expanded leaves using portable open gas exchange systems incorporating CO_2 and water vapor infra-red gas analyzers (LI-6800, LI-COR Biosciences, Lincoln, NE, USA).

Light was provided through an integrated LED light source and modulated fluorometer, incorporated into the head of the temperature- and humidity-controlled leaf measurement chamber (6 cm^2, LI-6800-01A, LI-COR Biosciences, Lincoln, NE, USA).

CO$_2$ and Light Response Curves

The response of CO_2 uptake (*A,* µmol CO_2 m^{-2} s^{-1}) to intercellular CO_2 concentration (*C_i,* µmol mol^{-1}) and *A* to photosynthetic photon flux density (PPFD) were measured twice during the experiment. Response curves were performed 47- days after sowing (from the 24th to the 27th of August 2020) and once again later in development at 61- days after sowing (from the 7th to the 10th of September 2020). Response curves were measured for each genotype once per each block (n = 12).

To examine the response of A to *C_i* (*A/C_i* curves), photosynthesis was measured at saturating light (2000 µmol m^{-2} s^{-1}) and CO_2 concentrations in the following order: 400, 250, 150, 100, 50, 400, 550, 700, 900, 1100, 1300, and 1500 µmol mol^{-1}. Additionally, the block temperature was set at 28°C, the average relative humidity was between 66% to 77%, and the vapor pressure deficit (VPD) at leaf temperature was between 0.79 kPa to 1.74 kPa. The gas exchange systems were matched before each curve and steady-state fluorescence (*F_s*) and maximal light-adapted fluorescence (*$F_{m'}$*) were recorded at each measured *C_i*.

The *apparent $V_{c, max}$* (µmol m^{-2} s^{-1}) and *apparent J_{max}* (µmol m^{-2} s^{-1}) were calculated utilizing the equations from von Caemmerer & Farquhar (1981). Due to the changes in ambient temperature throughout the day, the leaf temperature was variable (raw data in Supplementary Figure 3). Accordingly, the temperature response curves from Bernacchi et al. (2001), and Bernacchi et al. (2003) were applied to obtain the *apparent $V_{c, max}$* and *apparent J_{max}* at 28°C. The "apparent" term is used because the parameters are based on *C_i* instead of CO_2 concentration inside the chloroplast (*C_c*). The photorespiratory CO_2 compensation point (*Γ*,* µmol mol^{-1}), carboxylation efficiency (*CE,* µmol m^{-2} s^{-1} µbar^{-1}), and the maximum rate of CO_2 uptake in saturating light and CO_2 (*A_{max},* µmol m^{-2} s^{-1}) were calculated from the *A/C_i* curves that were fitted at 28°C. *CE* was the initial slope of curves with *C_i* ≤ 250 µmol mol^{-1}.

A nonlinear analysis with the Marquardt method (Moualeu-Ngangue et al., 2017) that uses the equations from the variable *J* method to calculate *g_m* (mol m^{-2} s^{-1}) (Harley et al., 1992) and equations from Caemmerer & Farquhar (1981) and Farquhar & von Caemmerer (1982) were then used to obtain *C_c* (µmol mol^{-1}), *$V_{c, max}$* and *J_{max}*. For this analysis, the scaling constant (*c*) and the enthalpies of activation (*$ΔH_a$*) to calculate the Michaelis constant of Rubisco for CO_2 (*K_c*; µmol mol^{-1}), the inhibition constant (*K_o*; µmol mol^{-1}), and *Γ** at 25°C were taken from Sharkey et al. (2007). Then, the *$V_{c, max}$*, *J_{max}*, and *g_m* were adjusted to 28°C using the equations in Bernacchi et al. (2001), (2002), and (2003).

The *Γ** adjusted (*Γ*_adjusted)* for *g_m* was calculated as in Furbank et al. (2009) and Walker and Cousins (2013): *Γ*_adjusted = Γ*+R_d / g_m*, where *R_d* is daytime respiration rate obtained from the *A/C_i* curves.

6

Light response curves (*A/Q* curves) were measured at ambient [CO_2] (400 µmol mol^{-1}) and the following PPFDs: 2000, 1700, 1400, 1100, 800, 600, 425, 250, 150, 100, 50, and 0 µmol m^{-2} s^{-1}. The gas exchange systems were matched before each curve and F_s and $F_{m'}$ were recorded at each PPFD. The *A/Q* curves were fitted for quantum efficiency (Φ_{PSII}), leaf CO_2 uptake in saturated light (A_{sat}, µmol m^{-2} s^{-1}), and light compensation point utilizing the {photosynthesis} R-package (Stinziano et al., 2021; R Core Team, 2020), which uses the Marshall et al. (1980) non-rectangular hyperbola model.

Diurnal Measurements

Diurnal measurements were made every two hours on September 3, 2020, from 8:00 through 18:00. On this day, sunrise was at approximately 6:23, while sunset was at approximately 19:20. One plant of each genotype was measured in each of the 12 blocks per timepoint (n = 12/genotype/timepoint). Within the cuvette, the flow rate was 500 µmol s^{-1}, [CO_2] was maintained at 400 µmol mol^{-1}, relative humidity was maintained at 70%, and actinic PPFD was 10% blue light. The PPFD and block temperature were changed at each time point to reflect ambient conditions throughout the day. The gas exchange systems were matched before each timepoint measurement, and F_s and $F_{m'}$ were logged. The parameters of *A*, stomatal conductance (g_{sw}, mol H_2O m^{-2} s^{-1}), C_i, and intrinsic water-use efficiency (*iWUE* = A/g_{sw}, µmol CO_2 mol H_2O^{-1}) throughout the course of a day were obtained from these data.

Confirmation of ictB expression

Leaf discs were collected into liquid N_2 the day following the diurnal measurements (September 4, 2020) from one plant per tobacco genotype per block (n = 12 per genotype). After the samples were ground, total RNA and protein were extracted from the same leaf discs using the NucleoSpin RNA/Protein Kit (Macherey-Nagel, http://www.mn-net.com). Once the protocol was completed, the RNA concentration was diluted to 200ng/uL.

cDNA was synthesized using 1 µg total RNA in 20 µl using the oligo-dT primer (Invitrogene) according to the protocol in the RevertAid Reverse Transcriptase kit (Fermentas, Life Sciences, UK). The cDNA was diluted 10 times. For semi-quantitative RT–PCR, 10 µl of cDNA in a total volume of 25 µl was used with HS VeriFi Mix (PCR Biosystems Ltd., UK) according to the manufacturer's recommendations. The PCR products were fractionated on 2.0% agarose gels. qPCR reactions were prepared with the 2x qPCRBIO SyGreen Mix Lo-ROX (PCR Biosystems Ltd., UK) with 1µl of cDNA and 0.5µM of each primer in a total volume of 10µl. The amplification reaction included 40 cycles of 5 s at 95 °C, 10 s at 60 °C, and 15 s at 72 °C. The expression level of *ictB* was normalized with the values obtained for the housekeeping gene for Protein phosphatase 2A (PP2A; Supplementary Figure 4). Primers in 5'-3' orientation used, were RT-PCR-ictB-Fw: AGCCAAACTGACGCTCTACC ; RT-PCR-ictB-Rv: CGCGACTGTAGGTGAGGATC; qPCR-ictB-Fw: GTTGGTTTTTGCCCTAGCGG; qPCR-ictB-Rv: TTGGTTGAGGCCGTAGACAC; qPCR-PP2A-Fw: GTGAAGCTGTAGGGCCTGAGC; qPCR-PP2A-Rv: CATAGGCAGGCACCAAATCC.

7

Determination of leaf carbon and leaf carbon isotopic composition

Leaf discs were collected on September 4, 2020. Samples were freeze-dried and ground. Then, a ~2 mg of each leaf sample was used to determine the carbon content (leaf C, %) and the carbon isotopic composition ($\delta^{13}C$, ‰) using an elemental analyzer (Costech 4010, Costech Analytical Technologies, Valencia CA USA) in conjunction with an isotope ratio mass spectrometer (DeltaV Advantage, Thermo Fisher Scientific, Bremen, Germany) on continuous flow. The carbon ratios were then measured relative to laboratory standards and calibrated relative to the international Vienna Pee Dee Belemnite (VPDB) standard.

Destructive Harvest and Biomass Quantification

All tobacco plants (~48 plants per genotype) were harvested on September 16, 2020, to obtain the total number of leaves, number of leaves on the main stem, total leaf area (cm^2), and stem height (cm) per plant. Total leaf area was measured using a leaf area meter (LI-3100C Area Meter, LI-COR Environmental, Lincoln, NE, USA). Biomass samples were dried to a constant weight at 50°C to determine leaf dry and stem dry weight (g plant^{-1}). The above-ground biomass was the combined sum of leaf and stem dry weight. Leaf area ratio (LAR, cm^2 g^{-1}) was determined dividing the total leaf area by the total above-ground biomass.

Statistical Analyses

After testing for normal distribution, homogeneity of variances by the Shapiro-Wilk test and Levine test, variables were analyzed with a mixed model ANOVA with or without repeated measurements. "Day" was the repeated measurement factor when a variable was collected multiple times throughout the season. The fixed effects were the genotype (tobacco lines), day, and their interactions while the block was the random effect. The Kenward–Roger method was used to calculate the degrees of freedom. Mean discrimination analysis was performed utilizing Tukey's honest significant difference (HSD) with significance determined as *p*-value ≤0.05. Statistical analyses and model-fitting for the *A/Q* curves and diurnal measurements were performed in R (version 4.01, R-Project). The rest of the analyses were done in SAS (version 9.4, SAS Institute Inc., Cary, NC, USA), by using the PROC UNIVARIATE procedure to assess for normality and for the discovery of outliers and by using the PRO MIXED procedure for the ANOVA. Pair-wise comparisons were done by the least square means test (*t*-test) with significance determined as a *p*-value ≤0.05.

8

RESULTS:

Confirmation of ictB expression in transgenic plants

The ictB transgenic lines used in this study are the same as those presented in Simkin et al, 2015. Semi-quantitative RT-PCR was used to detect the presence of the transcript in the ictB-expressing plant lines ictB1, ictB3, ictB4 and ictB6. No transcript was detected in wild type control plants and different levels of transgene expression were observed among transgenic lines, with ictB6 showing the highest transgene expression (Sup Fig. 6a). qPCR was performed to validate the differences in transgene expression between lines. No signal was detected in WT plants and ictB6 showed the highest transgene expression (Sup Fig. 6b) Both results are consistent and indicate that the ictB transgene is expressed in transgenic lines at different levels, and these results are also consistent with the data presented in Simkin et al 2015.

Gas exchange data: CO_2 response curves, light response curves, and diurnals

A/Q curves were measured to allow for the determination of parameters related to how efficiently the plant is utilizing light. A/Q curves were measured on 12 plants per line (n = 12). No significant differences were found between genotypes for A_{sat}, Φ_{PSII}, and light compensation point for any of the A/Q curve measurements throughout the season (Figure 1). While not significant, WT had one of the highest photosynthetic rates in the first set of *A/Q* curves but not in the second set (Figure 1). However, indicated differences were small (Figure 1).

The *A/C_i* curves were measured to determine parameters related to the biochemical performance and limitation of photosynthesis. These were also measured on 12 plants per line (n = 12). The *apparent $V_{c, max}$*, *apparent J_{max}*, *CE*, *A_{max}*, and *Γ^** in the transgenic lines were not significantly higher than the WT. The overall values of these parameters increased throughout the duration of the season, but without significant differences between lines (Figure 2, Figure 3). Exceptions were that ictB3 had a lower *apparent $V_{c, max}$* and *CE* than the WT, ictB1 and ictB4 during the first set of measurements (Figure 3). ictB3 had also a lower *Γ^** than the WT and ictB1 at the beginning of the season (Figure 3). By the end of the field season, ictB4 had an *apparent $V_{c, max}$* and *CE* that were lower than in ictB3 and ictB6 (Figure 3). When considering the parameters calculated based on C_c, $V_{c, max}$, J_{max}, and Γ^*_adjusted did not differ between the transgenic lines and the WT (Supplementary Figure 5). ictB3 was the only transgenic with a g_m lower than the WT, although the difference was only significant on one date (Supplementary Figure 5).

Finally, no significant differences were found between the genotypes for *A*, g_{sw}, C_i, and *iWUE* during the diurnal gas exchange measurement (Figure 4). While WT had the lowest overall *iWUE*, it was not significantly lower in the transgenic lines (Figure 4).

9

Leaf composition and biomass related traits

Leaf carbon content (leaf C) and $\delta^{13}C$ varied significantly among the measured genotypes (Figure 5). None of the transformants showed a leaf C content that was significantly different from the WT, however, ictB1 showed a significantly higher content than ictB4 (Figure 5). WT had the lowest value (most negative) for $\delta^{13}C$ although it only varied significantly from the ictB4 genotype (Figure 5). The $\delta^{13}C$ values from all the ictB genotypes were compared (mean value of -27.48‰) against the $\delta^{13}C$ in the WT (mean value of -27.88‰), showing a significantly more negative $\delta^{13}C$ in the WT (*p*-value = 0.040).

Significant differences were found among the genotypes for most measured biomass-related traits, including above-ground biomass, leaf dry and stem dry weights, total number of leaves, number of leaves on the main stem, total leaf area, and stem height (Figure 6; Supplementary Figure 6). Despite having the lowest total number of leaves, WT had one of the highest total above-ground biomasses, total leaf area, and leaf dry weights (Figure 6, Supplementary Figure 6). WT had significantly lower total number of leaves and number of leaves on the main stem than the ictB3 transformant. WT also had higher above-ground biomass, stem dry weight, leaf dry weight, total leaf area, and stem height than both ictB3 and ictB4 transformants (Figure 6; Supplementary Figure 6). Finally, the pair-wise comparisons for LAR did not detect significant differences between the lines (Figure 6).

DISCUSSION:

Previous reports of plants transformed with the *ictB* gene indicated higher photosynthesis and biomass compared to the wild-type (WT) plants from which they were derived (Lieman-Hurwitz et al., 2003; Lieman-Hurwitz et al., 2005; Simkin et al 2015; Hay et al 2017). However, most of these studies have been performed in controlled conditions and it is not clear if these promising improvements in plant productivity can translate to the crops in the field. For this reason, in this experiment we grew *ictB* tobacco plants in the field to evaluate if these transgenic plants have a higher photosynthetic efficiency than WT under field conditions. A total of four *ictB* transgenic lines were tested against tobacco WT plants from which they were derived; evaluated for more than 10 different photosynthetic parameters together with leaf composition and biomass traits (Supplementary Table 1).

The same transgenic lines were used previously in the greenhouse study of Simkin et al. (2015). In that experiment, overall higher photosynthesis, *apparent $V_{c, max}$*, *apparent J_{max}*, and g_{sw} were found in these *ictB* lines, resulting in more leaves and stem biomass. In this experiment, we did not find any photosynthetic parameter that was higher in *ictB* tobacco compared to the WT (Figure 1-4; Supplementary Figure 5). In contrast, *ictB* tobacco performed similarly to WT although one transgenic line (ictB3) had a lower *apparent $V_{c, max}$*, *CE*, and g_m than WT in at least one of the set of measurements (Figure 3; Supplementary Figure 5). The lower g_m in ictB3 indicated a higher restriction to the diffusion of CO_2 inside the chloroplast than WT. However, ictB3 did show a lower Γ^* which suggests an increased concentration of CO_2 around Rubisco. However, when Γ^* was adjusted to consider the effect

10

of g_m, $\Gamma^*\_adjusted$ did not indicate a higher amount of CO_2 around Rubisco in ictB3 or in any other *ictB* line compared to WT (Supplementary Figure 5). Previous studies of plants transformed with *ictB* have calculated Γ^* from A/C_i response curves, without account for g_m (Hay et al., 2017; Lieman-Hurwitz et al., 2003; Gong et al., 2015). The present study indicates the importance of calculating Γ^* based on C_c instead of C_i for studies where the calculation of this parameter can allow a better understanding any photosynthetic improvement achieved.

The values of *apparent $V_{c, max}$* and *apparent J_{max}* from this study were also obtained at 25°C (Supplementary Table 2) to compare them with the values obtained in Simkin et al. (2015) which were calculated at that temperature. In our field experiment, the *apparent $V_{c, max}$* at 25°C was between 95 to 145 µmol m^{-2} s^{-1} while the *apparent J_{max}* was between 195 to 290 µmol m^{-2} s^{-1}, considering both *ictB* lines and WT. These values are higher than the *apparent $V_{c, max}$* (between 70 to 90 µmol m^{-2} s^{-1}) and the *apparent J_{max}* (between 130 to 170 µmol m^{-2} s^{-1}) obtained in the greenhouse study of Simkin et al. (2015). It is possible that under the controlled growth conditions of the greenhouse differences could be apparent that were later eliminated in the field. Similarly, in an *ictB* soybean study (Hay et al., 2017), the *apparent $V_{c, max}$* and *apparent J_{max}* were not different from the WT when grown in the field under ambient CO_2 concentrations, however, soybean instantaneous photosynthesis and biomass did increase. It is important to note that soybean as a legume can have an adequate nitrogen supply throughout the whole growing season, which might have contributed to its carbon assimilation increase. In Ruiz-Vera et al. (2017), WT tobacco cv. Petit Havana, another tobacco cultivar with reduced sink capacity due to its determinate growth, grew at normal and high N soil fertilization conditions in the field. In that study, the values of *apparent $V_{c, max}$* and the *apparent J_{max}* increased further under the high N treatment at ambient CO_2 conditions. It might be that under field conditions, other factors like adequate nutrient supply and uptake or sink strength can influence the effect of the *ictB* gene in tobacco. Our results suggest that it is possible to maximize the photosynthetic performance of *ictB* plants over WT under conditions where parameters such as the amount of light, temperature, relative humidity, photoperiod, nutrients, and water availability can be controlled (e.g. conditions in the *ictB* tobacco greenhouse experiment in Simkin et al. (2015)) but this improvement might not always translate to field conditions.

The values for A and other parameters obtained from the A/C_i and A/Q curves were higher at the end of the season compared to the beginning of the season (Figure 1-3; Supplementary Figure 3). This trend corresponds with previous work in which values related to photosynthesis increase with leaf age (Bielczynski et al., 2017). This difference could have been influenced by the hotter temperatures during the days when the first set of measurements were carried out (~+5°C; Supplementary Figure 2) which could have also increased the water requirements of the plants. Previous studies suggest that *ictB* plants might have higher water use efficiency (WUE) than WT because A and g_m tend to be higher while g_{sw} does not change (Hay et al., 2017; Gong et al., 2015; Lieman-Hurwitz et al., 2003). In our experiment, *iWUE* was not significantly different between *ictB* tobacco and WT (Figure 4), which coincided with the lack of significant differences seen, in most of the cases, for A, g_{sw}

11

g_m and δ^{13}C. However, ictB4 did show significantly less negative δ^{13}C than WT, and a less negative δ^{13}C was indicated for ictB1 (Figure 5). The δ^{13}C of leaf tissue provides an integrated signal of the water use efficiency with which the carbon in that leaf was obtained. A less negative value indicates a higher water use efficiency, provided that g_m is not different between lines. These results suggest that the transformation with *ictB* may improve water use efficiency under field conditions, although scope may be limited (Figure 5).

The results regarding the effect of ictB on crop biomass production have so far been inconclusive. For example, in some cases ictB overexpressing plants have produced significantly greater biomass (Lieman-Hurwitz et al., 2003; Hay et al., 2017; Koester et al., 2021), while in other studies overexpression of ictB did not significantly alter biomass production (Gong et al., 2015). This suggests that the mechanism that underlies ictB may be greatly affected by environmental factors, and that an increase in crop productivity may only happen under certain conditions, although these conditions have yet to be identified. Here, there were no increases in biomass in *ictB* tobacco, on the contrary, some *ictB* lines (ictB3 and ictB4) had lower biomass (above-ground biomass, leaves biomass, and stem biomass; Figure 6) than the WT, probably because of the production of smaller leaves (total leaf area; Figure 5) and shorter plants (Supplementary Figure 6). This study did not measure root biomass; however, empirical observations in the previous greenhouse experiment indicated that *ictB* lines might have more root biomass than the WT (Simkin et al., 2015). Despite that, the effect of the *ictB* expression in plants remains unclear (Simkin et al., 2019), its effect might be enhanced when it is co-expressed with other genes like with some Calvin Benson cycle genes (Simkin et al., 2017). For example, higher dry biomass was observed in plants with the *ictB* gene together with the overexpression of sedoheptulose-1,7-bisphosphatase (SBPase) and fructose-1,6-bisphosphate aldolase (FBPase) (Simkin et al., 2017). Consequently, the impact of *ictB* on the improvement of photosynthesis and yield may be observed when it is part of a group of expressed genes rather than when it is expressed alone.

Future Applications for ictB overexpressing plants

Despite not finding a significant difference between the *ictB* transformants and the WT except possibly in water use efficiency, this study was done in one field season so the replication of our results in multiples seasons is unknown. Moreover, there is still promise in utilizing expression of this gene for improved crop productivity, particularly in controlled environments. While we did not find the significant differences in biomass that were reported in Simkin et al. (2015), it is possible that field environmental conditions, which differ heavily from potted plants in the constant conditions of greenhouses and growth cabinets, play a key role in whether plant transformed with *ictB* perform better relative to their WT. This, combined with the successes seen in greenhouse grown *ictB* transformants, could serve as encouragement for deploying this gene to improve plant productivity within the context of controlled environments. Indeed, as humans globally look to increase food production in more sustainable ways, greater emphasis has been placed on agriculture in greenhouses and vertical farming, both of which involve controlling the growing environment.

Other considerations that could be taken into account are the water status of the plant, temperature, and the age of the plant as all of these are factors that can play a role in how a transgene manifests itself in the field and to affect photosynthetic performance (Azcon-Bieto

et al., 1981). As of now, it is difficult to know the true potential of transformation of crop plants with *ictB*, especially as the function of the gene remains unknown (Simkin et al., 2019).

Drought and heat conditions adversely affect photosynthetic performance in crops, including increasing the photorespiratory CO_2 compensation point and decreasing Rubisco carboxylation or RuBP regeneration (Rensburg and Kruger, 1993; Antolin and Sanchez-Diaz, 1993; Flexas et al., 2009; Crous et al., 2013). Consequently, increases in temperature are associated with an increase in photorespiration in C_3 plants, which can lead to yield penalties of up to 36% in important food crops (Walker et al., 2016). Previously, it was shown that expression of *ictB* in plants resulted in a decrease of Γ^* (Lieman-Hurwitz et al., 2003; Hay et al. 2017). Testing ictB transformants under conditions that are known to affect CO_2 compensation point could help us to better understand the underlying function and see if improved performance is significantly associated with specific environmental factors. For example, if *ictB* transformants can maintain a lower Γ^* under drought or heat stress conditions, then it could be a promising application for the future, especially as temperature and drought stress are projected to increase with global climate change. However, as mentioned, further effort would need to be placed into understanding under which specific conditions *ictB* might be most beneficial.

SUPPLEMENTARY DATA:

Supplementary Figure 1. Layout of field experiment.

Supplementary Figure 2. Weather data for the growing season.

Supplementary Figure 3. Raw data for A/C_i curves.

Supplementary Figure 4. Semi-quantitative RT-PCR and qPCR results of transgenic lines.

Supplementary Figure 5. Comparison of $V_{c,max}$, J_{max}, g_m, and $\Gamma^*\_adjusted$ between transgenic lines and wildtype at 28° C.

Supplementary Figure 6. Stem height and number of leaves on the main stem.

Supplementary Table 1. Summary of traits measured, their abbreviations, and units.

Supplementary Table 2. Apparent $V_{c,max}$ and J_{max} at 25° C.

Author Contributions:

CR, TL, and SPL conceived the original research plans. AJS developed the ictB transformants used in this study, which was supported by KLB. CA and HG confirmed the expression of *ictB* in the plants used in this experiment. CR and TL designed the experiments. UMRZ and LGAS performed the gas exchange measurements and field harvest. UMRZ and LGAS analyzed the data and wrote the article with contributions from all other authors. CR agrees to serve as the corresponding author and respond to any relevant communication related to this project.

Conflicts of Interest: No conflicts of interest.

work was also supported by the Biotechnology and Biological Sciences Research Council (BBSRC) grant no. BB/J004138/1.

15

REFERENCES:

Antolín MC, Sánchez-Díaz M. 1993. Effects of Temporary Droughts on Photosynthesis of Alfalfa Plants. *Journal of Experimental Botany*, **44**, 1341-1349.

Azcón-Bieto J, Farquhar GD, Caballero A. 1981. Effects of temperature, oxygen concentration, leaf age and seasonal variations on the CO2 compensation point of Lolium perenne L. *Planta*, **152**, 497-504.

Bernacchi CJ, Pimentel C, Long SP. 2003. *In vivo* temperature response functions of parameters required to model RuBP-limited photosynthesis. *Plant, Cell & Environment*, **26**, 1419–1430.

Bernacchi CJ, Singsaas EL, Pimentel C, Portis ARJ, Long SP. 2001. Improved temperature response functions for models of Rubisco-limited photosynthesis. *Plant, Cell & Environment*, **24**, 253–259.

Bielczynski LW, Lacki MK, Hoefnagels I, Gambin A, Croce R. 2017. Leaf and Plant Age Affects Photosynthetic Performance and Photoprotective Capacity. *Plant Physiology*, **175**, 1634-1648.

Bonfil DJ, Ronen-Tarazi M, Sültemeyer D, Lieman-Hurwitz J, Schatz D, Kaplan A. 1998. A putative HCO_3^- transporter in the cyanobacterium *Synechococcus* sp. strain PCC 7942. *FEBS Letters*, **430**, 236-240.

Bunce J. 2018. Three Methods of Estimating Mesophyll Conductance Agree Regarding its CO_2 Sensitivity in the Rubisco-Limited C_i Range. *Plants*, **7**, 62. https://doi.org/10.3390/plants7030062

Crous KY, Quentin AG, Lin YS, Medlyn BE, Williams DG, Barton CVM, Ellsworth D. 2013. Photosynthesis of temperate Eucalyptus globulus trees outside their native range has limited adjustment to elevated CO_2 and climate warming. *Global Change Biology*, **19**, 3790-3807.

Erb TJ, Zarzycki J. 2018. A short history of RubisCO: the rise and fall (?) of Nature's predominant CO_2 fixing enzyme. *Current Opinion in Biotechnology*, **49**, 100-107.

Ermakova M, Danila FR, Furbank RT, von Caemmerer S. 2020. On the road to C4 rice: advances and perspectives. *The Plant Journal*, **101**, 940-950.

von Caemmerer S, Farquhar GD (1981) Some relationships between the biochemistry of photosynthesis and the gas exchange of leaves. *Planta*, **153**, 376-387.

Farquhar GD, von Caemmerer S. 1982. Modelling of photosynthetic response to environmental conditions. In: Lange OL, Nobel PS, Osmond CB, Ziegler H, eds. Physiological plant ecology II. Berlin, Heidelberg, Germany: Springer, 549–587.

Flexas J, Barón M, Bota J, Ducruet JM, Gallé A, Galmés J, Jiménez M, Pou A, Ribas-Carbó M, Sajnani C, Tomàs M, Medrano H. 2009. Photosynthesis limitations during water stress

16

acclimation and recovery in the drought-adapted Vitis hybrid Richter-110 (V. berlandieri·V. rupestris). *Journal of Experimental Botany*, **60**, 2361-2377.

FAO, IFAD, UNICEF, WFP and WHO. 2020. *The State of Food Security and Nutrition in the World 2020. Transforming food systems for affordable healthy diets. Rome*, FAO. https://doi.org/10.4060/ca9692en

Foley JA, Ramankutty N, Brauman KA, Cassidy ES, Gerber JS, Johnston M, Mueller ND, O'Connell C, Ray DK, West PC, Balzer C, Bennett EM, Carpenter SR, Hill J, Monfreda C, Polasky S, Rockström J, Sheehan J, Siebert S, Tilman D, Zaks DPM. 2011. Solutions for a cultivated planet. *Nature*, **478**, 337-342.

Furbank RT, von Caemmerer S, Sheehy J, Edwards GE. 2009. C4 rice: a challenge for plant phenomics. *Functional Plant Biology*, **36**, 845–859.

Gong HY, Li Y, Fang G, Hu DH, Jin WB, Wang ZH, Li YS. 2015. Transgenic rice expressing *Ictb* and *FBP/Sbpase* derived from cyanobacteria exhibits enhanced photosynthesis and mesophyll conductance to CO_2. *PLoS ONE,* **10**(10): e0140928. https://doi.org/10.1371/journal.pone.0140928.

Harley PC, Loreto F, Di Marco G, Sharkey TD. 1992. Theoretical considerations when estimating the mesophyll conductance to CO_2 flux by analysis of the response of photosynthesis to CO_2. *Plant Physiology*, **98**, 1429–1436.

Hay WT, Bihmidine S, Mutlu N, Hoang KL, Awada T, Weeks DP, Clemente TE, Long SP. 2017. Enhancing soybean photosynthetic CO_2 assimilation using a cyanobacterial membrane protein, ictB. *Journal of Plant Physiology*, **212**, 58-68.

Koester RP, Pignon CP, Kesler DC, Willison RS, Kang M, Shen Y, Priest HD, Begemann MB, Cook KA, Bannon GA, Oufattole M. 2021. Transgenic insertion of the cyanobacterial membrane protein ictB increases grain yield in Zea mays through increased photosynthesis and carbohydrate production. *PLoS ONE*, **16**(2), e0246359.

Lieman-Hurwitz J, Rachmilevitch S, Mittler R, Marcus Y, Kaplan A. 2003. Enhanced photosynthesis and growth of transgenic plants that express ictB, a gene involved in HCO_3^- accumulation in cyanobacteria. *Plant Biotechnology Journal*, **1**, 43-50.

Lieman-Hurwitz J, Asipov L, Rachmilevitch S, Marcus Y, Kaplan A. 2005. Expression of cyanobacterial *ictB* in higher plants enhanced photosynthesis and growth. In: Omasa K, Nouchi I, De Kok LJ, eds. Plant Responses to Air Pollution and Global Change. Tokyo: Springer, 133-138. https://doi.org/10.1007/4-431-31014-2_15

Long SP, and Bernacchi CJ. 2003. Gas exchange measurements, what can they tell us about the underlying limitations to photosynthesis? Procedures and sources of error. Journal of Experimental Botany, **54**, 2393-2401.

Long SP, and Ort DR. 2010. More than taking the heat: crops and global change. *Current Opinion in Plant Biology*, **13**, 241–248.

Long SP, Marshall-Colon A, Zhu XG. 2015. Meeting the Global Food Demand of the Future by Engineering Crop Photosynthesis and Yield Potential. *Cell*, **161**, 56-66.

Long BM, Hee WY, Sharwood RE, Rae BD, Kaines S, Lim YL, Nguyen ND, Massey B, Bala S, von Caemmerer S, Badger MR, Price GD. 2018. Carboxysome encapsulation of the CO_2-fixing enzyme Rubisco in tobacco chloroplasts. *Nature Communications*, **9**, 3570.

McGrath JM, Long SP. 2014. Can the cyanobacterial carbon-concentrating mechanism increase photosynthesis in crop species? A theoretical analysis. *Plant Physiology*, **164**, 2247-2261.

Mitchell PL, Sheehy JE. 2006. Supercharging rice photosynthesis to increase yield. *New Phytologist*, **171**, 688-693.

Moualeu-Ngangue DP, Chen T-W, Stützel H. 2017. A new method to estimate photosynthetic parameters through net assimilation rate–intercellular space CO_2 concentration ($A–C_i$) curve and chlorophyll fluorescence measurements. *New Phytologist*, **213**, 1543–1554.

Parry MA, Reynolds M, Salvucci ME, Raines C, Andralojc J, Zhu XG, Price GD, Condon AG, Furbank RT. 2011. Raising yield potential of wheat. II. Increasing photosynthetic capacity and efficiency. *Journal of Experimental Botany*, **62**, 453-467.

Pons TL, Flexas J, von Caemmerer S, Evans JR, Genty B, Ribas-Carbo M, Brugnoli E. 2009. Estimating mesophyll conductance to CO_2: methodology, potential errors, and recommendations, *Journal of Experimental Botany*, **60**, 2217 2234. https://doi.org/10.1093/jxb/erp081

Price GD, Pengelly JJL, Forster B, Du J, Whitney SM, von Caemmerer S, Badger MR, Howitt SM, Evans JR. 2013. The cyanobacterial CCM as a source of genes for improving photosynthetic CO_2 fixation in crop species. *Journal of Experimental Botany*, **64**, 753-768.

R Core Team. 2020. R: A language and environment for statistical computing. R Foundation for Statistical Computing, Vienna, Austria. URL http://www.R-project.org/

Ray DK, Ramankutty N, Mueller ND, West PC, Foley JA. 2012. Recent patterns of crop yield growth and stagnation. *Nature Communications*, **3**, 1293.

Ray DK, Mueller ND, West PC, Foley JA. 2013. Yield trends are insufficient to double global crop production by 2050. *PLoS ONE*, **8**, e66428

Rensburg LV, Krüger GHJ. 1993. Comparative Analysis of Differential drought Stress-induced Suppression of and Recovery in Carbon Dioxide Fixation: Stomatal and Non-stomatal Limitation in Nicotiana tabacum L. *Journal of Plant Physiology*, **142**, 296-306.

Ruiz-Vera UM, De Souza AP, Long SP, Ort DR. 2017. The role of sink strength and nitrogen availability in the down-regulation of photosynthetic capacity in field-grown Nicotiana tabacum L. at elevated CO2 concentration. *Frontiers in Plant Science*, **8**, 998. https://doi.org/10.3389/fpls.2017.00998

18

Sharkey TD, Bernacchi CJ, Farquhar GD, Singsaas EL. 2007. Fitting photosynthetic carbon dioxide response curves for C3 leaves. *Plant, Cell & Environment*, **30**, 1035–1040.

Simkin AJ, McAusland L, Headland LR, Lawson T, Raines CA. 2015. Multigene manipulation of photosynthetic carbon assimilation increases CO_2 fixation and biomass yield in tobacco. *Journal of Experimental Botany*, **66**, 4075-4090.

Simkin AJ, Lopez-Calcagno PE, Davey PA, Headland LR, Lawson T, Timm S, Bauwe H, Raines CA. 2017. Simultaneous stimulation of sedoheptulose 1,7-bisphosphatase, fructose 1,6-bisphophate aldolase and the photorespiratory glycine decarboxylase h-protein increases CO_2 assimilation, vegetative biomass and seed yield in Arabidopsis. *Plant Biotechnology Journal*, **15**, 805-816.

Simkin AJ, Lopez-Calcagno PE, Raines CA. 2019. Feeding the world: Improving photosynthetic efficiency for sustainable crop production. *Journal of Experimental Botany*, **70**, 1119-1140.

Tcherkez GGB, Farquhar GD, Andrews TJ. 2006. Despite slow catalysis and confused substrate specificity, all ribulose bisphosphate carboxylases may be nearly perfectly optimized. *Proceedings of the National Academy of Sciences of the United States of America*, **103**, 7246-7251.

Tilman D, Balzer C, Hill J, Befort BL. 2011. Global food demand and the sustainable intensification of agriculture. *Proceedings of the National Academy of Sciences of the United States of America*, **108**, 20260-20264.

Walker BJ, VanLoocke A, Bernacchi CJ, Ort DR. 2016. The Costs of Photorespiration to Food Production Now and in the Future. *Annual Review of Plant Biology*, **67**, 107-129.

Xu M, Bernát G, Singh A, Mi H, Rögner M, Pakrasi HB, Ogawa T. 2008. Properties of mutants of *Synechocystis* sp. strain PCC 6803 lacking inorganic carbon sequestration systems. *Plant and Cell Physiology*, **49**, 1672-1677.

Yang S-M, Chang C-Y, Yanagisawa M, Park I, Tseng T-H, Ku MSB. 2008. Transgenic Rice Expressing Cyanobacterial Bicarbonate Transporter Exhibited Enhanced Photosynthesis, Growth and Grain Yield. In: Allen JF, Gantt E, Golbeck J, Osmond B, eds. Photosynthesis. Energy from the Sun. Dodrecht: Springer, 1243-1246. https://doi.org/10.1007/978-1-4020-6709-9_268.

Zhu XG, Long SP, Ort DR. 2008. What is the maximum efficiency with which photosynthesis can convert solar energy into biomass? *Current Opinion in Biotechnology*, **2**, 153-159.

FIGURE LEGENDS:

Figure 1. CO_2 uptake (A) response to change in light ($PPFD$) in ictB tobacco transformants (ictB1, ictB3, ictB4, ictB6) and wildtype (WT) tobacco. The light response curves were measured in ambient [CO_2] conditions (~400 mol mol^{-1}). Each point is the mean (± SE) of twelve plants.

Figure 2. CO_2 uptake (A) response to change in intercellular CO_2 concentration (C_i) fitted at 28ºC in *ictB* tobacco transformants (ictB1, ictB3, ictB4, ictB6) and wildtype (WT) tobacco. The CO_2 response curves were measured in saturating light conditions (2000 μmol m^{-2} s^{-1}). Raw data is provided in Supplementary Figure 2.

Figure 3. The "apparent" maximum rate of carboxylation (*apparent $V_{c, max}$*), the "apparent" maximum rate of electron transport (*apparent J_{max}*), the compensation point (Γ^*), carboxylation efficiency (*CE*) and the maximum rate of CO_2 uptake in saturating light and CO_2 (A_{max}) based on *A/C_i* curves at 28º C for *ictB* tobacco transformants and wildtype (WT) tobacco. Each point is the mean (± SE) of eight to twelve plants per genotype. Results of the complete block analysis of variance (ANOVA) for the season and for each day of measurements are at the top of each panel. Pair-wise comparisons (*t*-test) are indicated with letters on top of the bars; transformants with different letters represent statistically significant differences ($p < 0.05$).
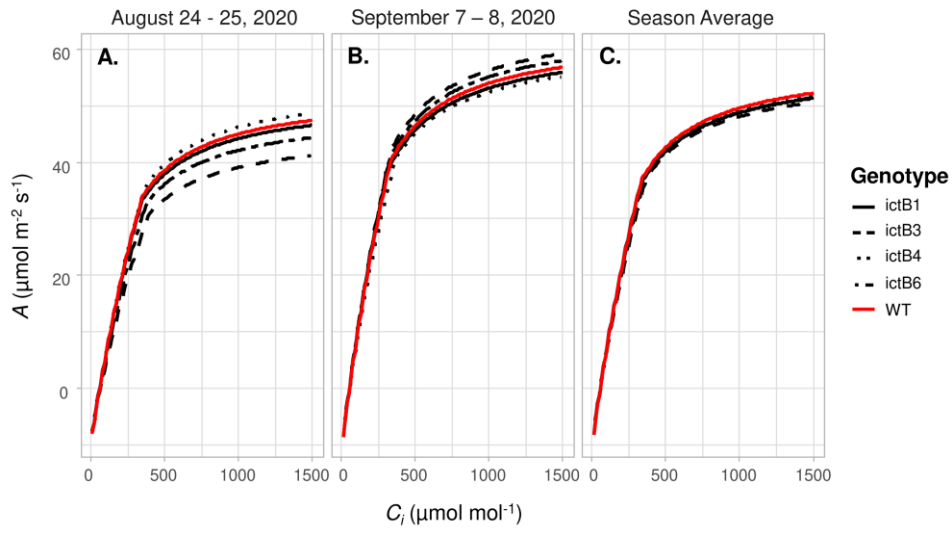
Figure 4. Photosynthetic parameters CO_2 uptake (A), stomatal conductance (g_{sw}), intrinsic water-use efficiency (*iWUE = A/g_s*), and intercellular CO_2 concentration (C_i) measured in diurnal measurement in five genotypes, 4 of which (ictB1, ictB3, ictB4, ictB6) being transgenic transformants expressing inorganic-carbon transporter B (ictB). Diurnal measurements were made every two hours on September 3, 2020, from 8:00 through 18:00. On this day, sunrise was at approximately 6:23, while sunset was at approximately 19:20. Each point is the mean (± SE) of twelve plants. Analysis of variance (ANOVA) results are at the bottom of each panel, with significance determined as a *p*-value ≤0.05. The ≈ symbol denotes an axis break.

Figure 5. Leaf carbon content and leaf carbon isotope composition (δ^{13}C). Each bar is the mean (± SE) of ~12 samples. Results of the complete block analysis of variance (ANOVA) for the season and for each day of measurements are at the top of each panel. Pair-wise comparisons (*t*-test) are indicated with letters on top of the bars; transformants with different letters represent statistically significant differences ($p < 0.05$).

Figure 6. Biomass data collected from destructive harvest of the five genotypes measured. Each bar is the mean (± SE) of ~48 plants. Results of the complete block analysis of variance (ANOVA) for the season and for each day of measurements are at the top of each panel. Pair-wise comparisons (*t*-test) are indicated with letters on top of the bars; transformants with different letters represent statistically significant differences ($p < 0.05$).

20

Figure 1. CO_2 uptake (A) response to change in light ($PPFD$) in *ictB* tobacco transformants (ictB1, ictB3, ictB4, ictB6) and wildtype (WT) tobacco. The light response curves were measured in ambient [CO_2] conditions (~400 mol mol-1). Each point is the mean (± SE) of twelve plants.
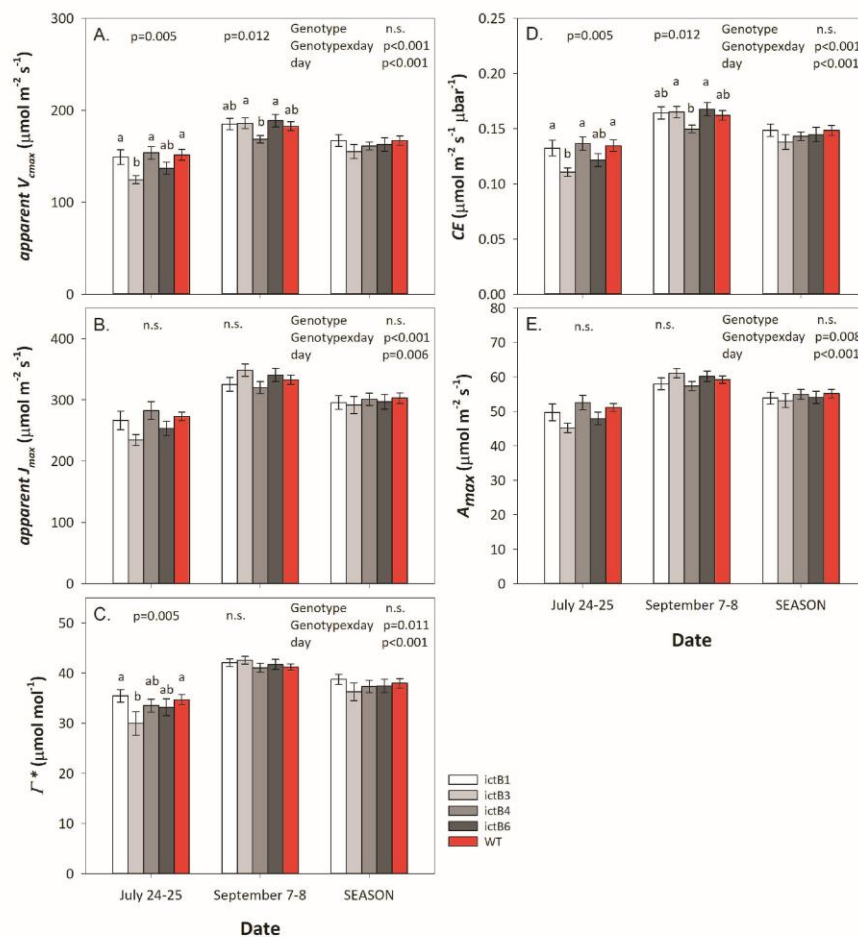
Figure 2. CO_2 uptake (*A*) response to change in intercellular CO_2 concentration (*C_i*) fitted at 28°C in *ictB* tobacco transformants (ictB1, ictB3, ictB4, ictB6) and wildtype (WT) tobacco. The CO2 response curves were measured in saturating light conditions (2000 µmol m-2 s^{-1}). Raw data is provided in Supplementary Figure 2.
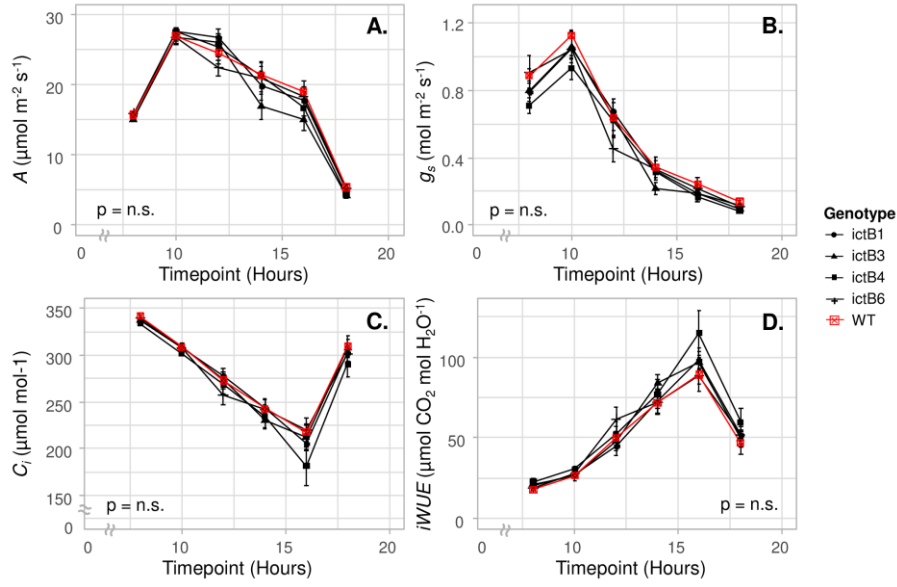
Figure 3. The "apparent" maximum rate of carboxylation (*apparent $V_{c, max}$*), the "apparent" maximum rate of electron transport (*apparent J_{max}*), the compensation point (Γ^*), carboxylation efficiency (*CE*) and the maximum rate of CO_2 uptake in saturating light and CO_2 (*Amax*) based on A/C_i curves at 28º C for *ictB* tobacco transformants and wildtype (WT) tobacco. Each point is the mean (± SE) of eight to twelve plants per genotype. Results of the complete block analysis of variance (ANOVA) for the season and for each day of measurements are at the top of each panel. Pair-wise comparisons (*t*-test) are indicated with letters on top of the bars; transformants with different letters represent statistically significant differences (*p* < 0.05).

Figure 4. Photosynthetic parameters CO_2 uptake (A), stomatal conductance (g_{sw}), intrinsic water-use efficiency ($iWUE = A/g_s$), and intercellular CO_2 concentration (C_i) measured in diurnal measurement in five genotypes, 4 of which (ictB1, ictB3, ictB4, ictB6) being transgenic transformants expressing inorganic-carbon transporter B (ictB). Diurnal measurements were made every two hours on September 3, 2020, from 8:00 through 18:00. On this day, sunrise was at approximately 6:23, while sunset was at approximately 19:20. Each point is the mean (± SE) of twelve plants. Analysis of variance (ANOVA) results are at the bottom of each panel, with significance determined as a p-value ≤0.05. The ≈ symbol denotes an axis break.
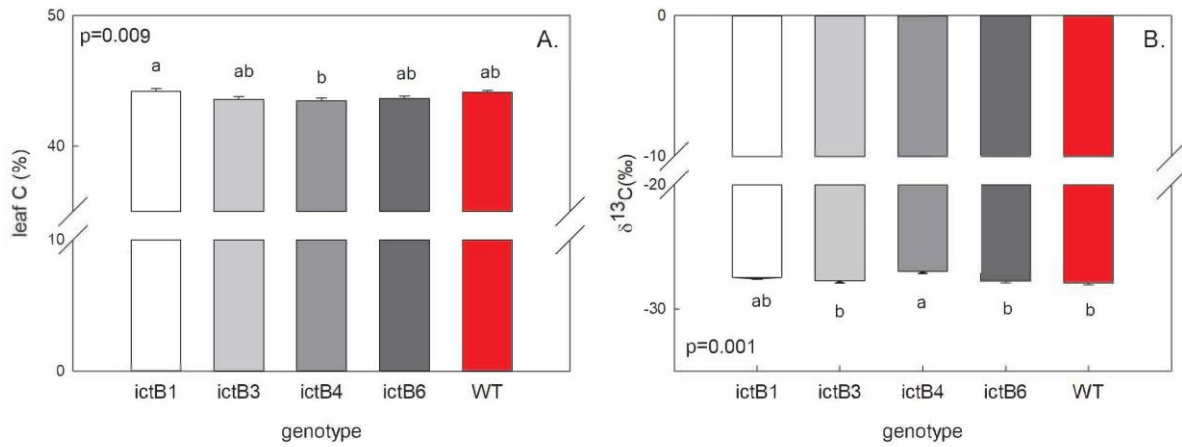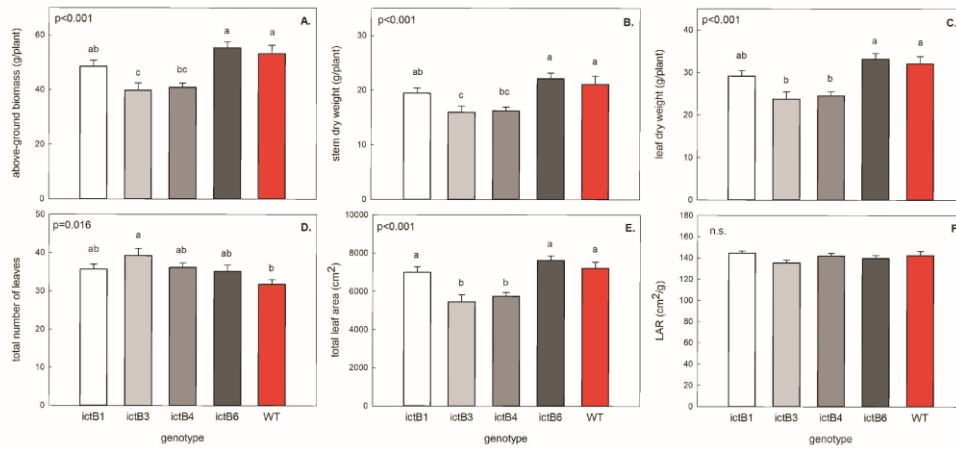
Figure 5. Leaf carbon content and leaf carbon isotope composition (δ^{13}C). Each bar is the mean (± SE) of ~12 samples. Results of the complete block analysis of variance (ANOVA) for the season and for each day of measurements are at the top of each panel. Pair-wise comparisons (t-test) are indicated with letters on top of the bars; transformants with different letters represent statistically significant differences ($p < 0.05$).

25

Figure 6. Biomass data collected from destructive harvest of the five genotypes measured. Each bar is the mean (± SE) of ~48 plants. Results of the complete block analysis of variance (ANOVA) for the season and for each day of measurements are at the top of each panel. Pair-wise comparisons (t-test) are indicated with letters on top of the bars; transformants with different letters represent statistically significant differences ($p < 0.05$).